Biomaterials 34 (2013) 6261–6271

Contents lists available at SciVerse ScienceDirect

Biomaterials

journal homepage: www.elsevier.com/locate/biomaterials

The effect of intracellular protein delivery on the anti-tumor activity of recombinant human endostatin

Junghee Lim [a,1], Tam Duong [b,1], Guewha Lee [a], Baik Lin Seong [c], Wael El-Rifai [d,e], H. Earl Ruley [f], Daewoong Jo [a,b,d,*]

[a] ProCell R&D Institute, ProCell Therapeutics, Inc., Seoul 151-050, Republic of Korea
[b] Department of Biomedical Sciences, Chonnam National University Medical School, Kwangju 501-746, Republic of Korea
[c] Department of Biotechnology and Translational Research Center for Protein Function Control, Yonsei University, Seoul 120-749, Republic of Korea
[d] Department of Surgery, Vanderbilt University School of Medicine, Nashville, TN 37232, USA
[e] Department of Cancer Biology, Vanderbilt University School of Medicine, Nashville, TN 37232, USA
[f] Department of Pathology, Microbiology & Immunology, Vanderbilt University School of Medicine, Nashville, TN 37232, USA

ARTICLE INFO

Article history:
Received 13 March 2013
Accepted 6 May 2013
Available online 25 May 2013

Keywords:
Endostatin
Macromolecule transduction domain
Protein therapy
Intracellular delivery

ABSTRACT

Endostatin (ES), a 20 kDa protein derived from the carboxy-terminus of collagen XVIII is a potent angiogenesis inhibitor, but clinical development has been hindered by poor clinical efficacy and insufficient functional information from which to design agents with improved activity. The present study investigated protein uptake by cells as a determinant of ES activity. We developed a cell-permeable ES protein ($HM_{73}ES$) with enhanced capacity to enter cells by adding a macromolecule transduction domain (MTD). $HM_{73}ES$ inhibited angiogenesis-associated phenotypes in cultured endothelial cells [as assessed by tube formation, wound-healing, cell proliferation and survival assays]. These effects were accompanied by reductions in MAPK signaling (ERK phosphorylation), and in β-Catenin, c-Myc, STAT3, and VEGF protein expression. The cell-permeable ES displayed greater tissue penetration in mice and suppressed the growth of human tumor xenografts to a significantly greater extent than ES protein without the MTD sequence. Our results suggest that anti-angiogenic activities of native ES are limited at the level of protein uptake and/or subcellular localization, and that much of the activity of ES against tumors depends on one or more intracellular functions. This study will inform future efforts to understand ES function(s) and suggest strategies for improving ES-based cancer therapeutics.

1. Introduction

Angiogenesis, the process of blood vessel formation, is essential for tumor growth and therefore provides an attractive target for anti-cancer therapies. Toward this end, a number of agents targeting angiogenesis have entered clinical trials [1,2]. These trials confirm that anti-angiogenesis agents can produce measureable clinical benefits (primarily progression-free interval) when used in combination with other therapies, and consequently, the most effective have been approved for use against selected tumor types [1,2]. However, with limited impact on overall survival and toxicity profiles that limit application [3], the therapeutic benefits of targeting angiogenesis havefallen short of expectations.

Endostatin (ES), a 20 kDa protein derived from carboxy-terminus of collagen XVIII, was among the first endogenous proteins identified with anti-angiogenic activity as assessed by in vitro effects on endothelial cell proliferation, survival and tube formation [4]. Interest in Endostatin, and indeed in angiogenesis as a therapeutic target, was spurred by a report describing tumor inhibition in mice treated with high doses of recombinant endostatin [5]. ES moved quickly into clinical trials; however, clinical development ended in the U.S. in 2003 due to limited efficacy and problems with protein formulation and application [1]. Clinical development later resumed in China using a reformulated histidine-tagged protein (Endostar®) with improved solubility and activity [1,6]. However, current clinical development of ES continues to be hampered by insufficient understanding about the mechanism(s) by which the protein inhibits angiogenesis, despite an extensive literature on

* Corresponding author. Department of Surgery, Vanderbilt University School of Medicine, 760 PRB, 2220 Pierce Avenue, Nashville, TN 37232, USA. Tel.: +1 615 322 8207; fax: +1 615 322 7852.
E-mail address: dae-woong.jo@vanderbilt.edu (D. Jo).
[1] These two authors contributed equally to this work.

0142-9612/$ – see front matter © 2013 Elsevier Ltd. All rights reserved.
http://dx.doi.org/10.1016/j.biomaterials.2013.05.011

receptors, targets, and cellular processes implicated in ES function [7–20].

Externally administered ES is internalized by endothelial cells, and the internalization appears to be important if not essential for the biological activities of the protein [7,9,18,21,22]. The role of individual ES binding proteins in protein uptake is unclear, since ES entry appears to employ multiple-and competing-pathways, including clatherin and lipid raft/caveolin-dependent processes. We suspect absorptive endocytosis contributes to basal ES uptake, as is commonly observed with basic proteins that, like ES [8,23–25], have affinity for cell surface heparin sulfate proteoglycans [26,27]. ES induces lipid raft clustering, a process suppressed by cholesterol depletion [28,29]. Cholesterol depleting agents also appear to change the default route of ES entry from a lipid raft- to a clatherin-dependent pathway, and enhance anti-angiogenic activity as assessed by tube formation and wounded-monolayer healing assays [21].

Although correlative, these observations led us to make several predictions about ES activity. First, ES internalization and/or cytoplasmic delivery are important for anti-angiogenic activity. This implicates intracellular targets in ES function; thus, optimal ES activity requires more than signaling from proteins on the cell surface. Second, ES uptake and/or cytoplasmic delivery are intrinsically limited; thus, simply exposing cells to native ES willnot result in maximum biological activity. The reliance on inefficient uptake mechanisms would also explain why tumor inhibition requires far higher concentrations of ES (0.2–20 mg/ml) than are present in the circulation (40–100 ng/ml) [30]. To test these predictions, we employed macromolecule intracellular transduction technology (MITT) to deliver human recombinant ES protein directly into cultured endothelial cells and to target human tumor xenografts in mice. MITT exploits the ability of hydrophobic macromolecule transduction domains (MTDs) to facilitate the transfer of peptides and proteins across the plasma membrane [31–33]. If our predictions are correct, then MTD-modified ES should display enhanced anti-angiogenic activity when compared to an identical protein lacking the MTD sequence by circumventing entry bottlenecks that limit cytoplasmic uptake of native ES. Moreover, since MITT-based protein therapies have been used in animals to protect against lethal inflammatory agonists [34–37], suppress pulmonary metastases [38] and inhibit subcutaneous tumor xenografts [31,39], we expected the MTD-modified ES would exhibit enhanced tissue penetration and anti-tumor activity as compared to unmodified ES.

2. Materials and methods

2.1. Derivation of MTD56 and MTD73

MTD56 and MTD73 were derived from predicted signal peptides (1–22 amino acid: MKVLLAAALIAGSVFFLLLPGP and 1 to 22: MMTPMWISLFKVLLLLFAFFAT, respectively) from the *Homo sapiens* P23274 (peptidyl-prolylcis-trans isomerase B precursor) and *Drosophila melanogaster* AAA17887 (spatzle) proteins, respectively. The sequences were modified by removing nonpolar, hydrophilic, and positively charged residues. In addition, other amino acids were replaced with alanine or proline to enhance bending and predicted alpha-helical structure (VLLAAALIAVLLLPP and PILVLLLLA, respectively), and the sequences were shortened to produce the final MTD56 (VLLAAALIA) and MTD73 (PVLLLLA) sequences (Supporting Information Table S1). The relative content of helix, sheet, and coil conformations was calculated using the ptraj program. Both MTD sequences hadalpha-helical secondary structure.

2.2. Construction of expression vectors for MTD-fused EGFP and MTD-fused endostatin

For recombinant proteins, the 2 MTDs were empirically chosen based on their relative cell permeability (1.4 and 2.7 fold) compared to a reference domain–membrane translocating sequence from Fibroblast Growth Factor 4 (FGF4 MTS: AAVLLPVLLAAP) assessed using an EGFP reporter protein. MTD56 and MTD73 were inserted in coding sequence of EGFP (E) and cloned into the *Escherichia coli* expression plasmid pET-28a(+) (Novagen, Darmstadt, Germany). Positive (FGF4-derived MTS: AAVLLPVLLAAP) and negative controls (unrelated peptide: SANVEPLERL) were also fused to EGFP.

These 2 MTDs used for development of 6 recombinant proteins by attaching to the N-terminus, to the C-terminus or to both ends of full-length endostatin (2 MTDs × 3 different structures = 6 MTD-fused proteins + 1 MTD-free control protein). Among them, we chose 3 endostatin proteins with N-, C- and both-terminal fused to MTD56, and 1 protein with N-terminal fused to MTD73 because these proteins were the most soluble and produced the highest when expressed in *E. coli*.

PCR primers for recombinant endostatin were HES-5′ (CCG CAT ATG CAC AGC CAC CGC GAC TTC CAG CCG GTG), HES-3′ (CCG CAT ATG CTA CTT GGA GGC AGT CAT GAA GCT GTT), $HM_{56}ES$-5′ (CCG CAT ATG GTG CTG CTG GCG GCGGCG CTG ATT GCG CAC AGC CAC CGC GAC TTC CAG CCG GTG), $HESM_{56}$-3′ (CCG CAT ATG CTA CGC AAT CAG CGC CGCCGC CAG CAG CAC CTT GGA GGC AGT CAT GAA GCT GTT), $HM_{73}ES$-5′ (CCG CAT ATG CCG GTG CTG CTGCTGCTG GCG CCG CAC AGC CAC CGC GAC TTC CAG CCG GTG) and HEM_{73}-3′ (CCG CAT ATG CTA CGG CGC CAG CAGCAGCAG CAC CGG CTT GGA GGC AGT CAT GAA GCT GTT). The proteins include vector-derived sequences (MGSSHHHHHHSSGLVPRGSM), which include a 6xHis tag (underlined) and thrombin cleavage site (double underline) appended to the N-terminus.

2.3. Purification of recombinant MTD-fused proteins

Proteins were purified from *E. coli* BL21-CodonPlus (DE3) cells grown to an A_{600} of 0.6 and induced for 2 h with 0.7 mM IPTG. 6xhistidine-tagged recombinant proteins were purified under denaturing conditions as directed by the supplier of the affinity matrix (Qiagen, Hilden, Germany) and refolded by dialyzing them against refolding buffer (0.55 M guanidine HCl, 0.44 M L-arginine, 50 mM Tris-HCl, 150 mM NaCl, 1 mM EDTA, 100 mM NDSB, 2 mM reduced glutathione, and 0.2 mM oxidized glutathione) at 4 °C for 48 h to remove the denaturing agent and dialyzed against a 7:3 mix of RPMI 1640 (Invitrogen, Grand Island, NY) and HBSS (Hank's balanced salt solution) supplemented with 5% glycerol and 0.1% CHAPS (Sigma–Aldrich, St. Louis, MO), at 4 °C for 9 h. Purified proteins contained low levels of endotoxin (<0.1 μg/mg) as determined by the limulus amebocyte lysate assay (Associates of Cape Cod, Inc., East Falmouth, MA).

Recombinant proteins were named using the following convention: H, E, ES and M stand for the His tag; EGFP, Endostatin and MTD, respectively. 6xHistidine-tagged recombinant Endostatin proteins were HES (His-Endostatin), $HM_{56}ES$ (His-MTD56-Endostatin), $HESM_{56}$ (His- Endostatin-MTD56), $HM_{56}ESM_{56}$ (His-MTD56-Endostatin-MTD56) and $HM_{73}ES$ (His-MTD73-Endostatin).

2.4. Analysis of cell-permeable ES uptake by cultured cells

For quantitative cell permeability, the recombinant EGFP proteins were conjugated to FITC according to the manufacturer's instructions (Pierce Chemical, Rockford, IL). RAW 264.7 cells were treated with 10 μM FITC-labeled proteins for 1 h at 37 °C, washed with cold PBS three times, treated with proteinase K (10 μg/ml) for 20 min at 37 °C to remove cell-surface bound proteins and subjected to fluorescence-activated cell sorting (FACS) analysis (FACSCalibur; BD, Franklin Lakes, NJ).

For visual cell permeability, NIH3T3 cells were treated with 10 μM FITC-conjugated recombinant proteins for 30 min or 1 h at 37 °C, washed with cold PBS three times, and treated with proteinase K (10 μg/ml) for 20 min at 37 °C. Treated cells were counterstained with the nuclear fluorescent stain propidium iodide (PI; Sigma–Aldrich, St. Louis, MO) at a concentration of 1 μg/ml or the cell membrane stain FM4-64 (Molecular Probes, Grand Island, NY) at a concentration of 5 μg/ml and washed with cold PBS three times. The intracellular localization of the fluorescent signal was determined by confocal laser scanning microscopy.

2.5. Analysis of systemic protein delivery in mice

Cells from human cancer lines, HCT116 and A549 were injected subcutaneously into the right legs of seven-week old mice (Central Lab. Animal Inc., Seoul) to initiate tumor formation.300 μg of FITC-labeled endostatin recombinant proteins (HES or $HM_{73}ES$) was administered to wild type Balb/c mice or tumor bearing Balb/c nu/nu mice after the tumors had reached 60–80 mm^3 in size. Two hours later, the mice were sacrificed, and liver, kidney, spleen, lung, heart, brain and tumor tissuesamples were embedded with an OCT compound (Sakura, Alphen an den Rijn, Netherlands), frozen, and then sectioned to a thickness of 14 μm. The tissue specimens were mounted on a glass slide and observed by fluorescence microscopy (Nikon, Tokyo, Japan).

2.6. Western blot analysis

Human umbilical vein endothelial cells (HUVECs) (Bio4You, Seoul, Korea) were maintained at 37 °C in a 5% CO_2 atmosphere of 2% gelatin coated dishes in M199 medium (300 mg/l L-glutamine, 2.2 g/L $NaHCO_3$, 25 mM HEPES, 10 unit/ml heparin, 20 ng/ml bFGF, 20% heat inactivated FBS, and 1% streptomycin/penicillin). The cells were cultured overnight in a serum-free medium, washed with phosphate-buffered saline (PBS) and treated with 10 μM recombinant proteins for 1 h. The cultures were

washed with PBS and returned to normal growth conditions for 2 h to analyze ERK phosphorylation, 8 h to measure β-Catenin and STAT3 expression, or 12 h to monitor c-Myc and VEGF expression. 5×10^6 cells were lysed in 100 μl 20 mM HEPES, pH 7.2, 1% triton-X100, 10% glycerol on ice for 30 min; the lysates were centrifuged at 4 °C for 20 min at 12,000 rpm and 50 μl of supernatants were subjected to western blot analysis as described previously. Anti- β-Catenin, c-Myc, STAT3, VEGF antibodies were purchased from Santa Cruz Biotechnology (Santa Cruz, CA). Anti- phospho-ERK1/2 and phospho-MEK1/2 antibodies were from Abcam (Cambridge, MA) and Cell Signaling (Danvers, MA), respectively, and goat anti-mouse IgG-HRP and goat anti-rabbit IgG-HRP were from Santa Cruz Biotechnology (Santa Cruz, CA).

2.7. Wound healing assay

Confluent HUVEC monolayers were treated with 10 μM HES or HM_{73}ES for 1 h in serum-free medium. The cells were washed twice with PBS, and the monolayer at the center of the well was "wounded" by scraping with a pipette tip and the recovery of the monolayer was monitored by phase contrast microscopy.

2.8. Tube formation assay

HUVECs were suspended in the pre-existing medium (M199) supplemented with 0.1% BSA. A total of 500 μl of M199 medium was added to each well of the BD Matrigel™ Matrix 12-well plate (BD Biosciences, San Jose, CA), and the cell suspension was inoculated. Next, each well was treated with 2.5, 5, 10, 15, 20 μM protein (HES or HM_{73}ES) for 16 h in M199 medium. The cells cultured on the plate were fixed in HBSS medium containing 1% paraformaldehyde and then stained with 10 μM calcein AM agent (BioVision, Milpitas, CA) for 30 min. The cells were then washed with PBS and observed by optical and fluorescence microscopy. The number of branch points was quantified by MetaMorph Imaging Series software (Universal Imaging, Bedford Hills, NY).

2.9. DNA content analysis

HUVECs were cultured in complete M119 medium with 50 ng/ml basic-FGF. The cells were treated with 2 μM protein (HES or HM_{73}ES) for 24 or 48 h. After the treatment, cells were washed twice with cold PBS and re-suspended in 200 μl cold PBS, fixed in cold 70% ethanol, washed with cold PBS twice and re-suspended in PI master mix (PI 40 μg/ml, DNase-free RNase 100 μg/ml in PBS) at a final cell density of 0.5×10^6 cell/ml. The cell mixtures were incubated at 37 °C for 30 min prior to analysis by flow cytometry.

2.10. Apoptosis and cytotoxicity assays

HUVEC, A549, MDA-MB-231 and HCT116 cell lines were purchased from the Korean Cell Line Bank (Seoul, Korea) and maintained as recommended by the supplier. The biological activities of the cell lines (A549, MDA-MB-231 and HCT116) were authenticated by in vivo metastasis and/or tumor growth in Balb/c nu/nu mice. All cell lines were negative for mycoplasma as assessed by using MycoALERT (2009; Lonza).HUVEC, A549, MDA-MB-231 and HCT116 cells were treated with recombinant proteins for varying times in the absence of serum, washed twice with cold PBS and re-suspended in 1× binding buffer (10 mM HEPEPS, 140 mM NaCl, 25 mM $CaCl_2$, pH 7.4) at a concentration of 1×10^6 cells/ml and stained with annexin V as instructed by the supplier (BD Biosciences, San Jose, CA) and analyzed within 1 h on a FACSCalibur.

NIH3T3 cells were with treated 10 μM protein (HES or HM_{73}ES) for 8 h. The cells were fixed and stained by the addition of 0.4% (w/v) Sulforhodamine Bin 1% acetic acid solution, followed by measurement at 570 nm with a spectrophotometer.

2.11. Xenograft tumor models

Five-week old Balb/c nu/nu mice (Central Lab. Animal Inc., Seoul, Korea) were subdivided into 3 groups of 5–6 mice each. 1×10^7 HCT116 or A549 cells (Korean Cell Line Bank, Seoul, Korea), were administered to the left upper back of the mouse via subcutaneous injection. From the day when the tumor size was measured as 60–80 mm^3 (width^2 × length × 0.52), proteins (HES or HM_{73}ES) or diluent (PBS) were administered daily (200–300 μg/mouse, 200 μl) by subcutaneous (proximal to the tumor) or intravenous injection for 21 days. Tumor size was monitored by measuring the longest (length) and shortest dimensions (width) once a day with a dial caliper, and tumor volume was calculated as width^2 × length × 0.5.

Formalin-fixed and paraffin-embedded sections (5-μm thick) of solid tumors obtained from mice were stained with hematoxylin and eosin (H&E). Tumor sections were incubated with primary antibody against vascular endothelial cell–specific marker 4A11 (Abcam, Cambridge, MA) and goat anti-mouse IgG-HRP (Biogenex, Fremont, CA) at 25 °C for 30 min each, washed three times with PBS and stained with diaminobenzidinete trahydrochloride (Biogenex, Fremont, CA). Subsequently, the section was washed with distilled water and counter-stained with hematoxylin.

2.12. Statistical analysis

All experimental data obtained using cultured cells were expressed as means ± S.D. For the tube formation assay, annexin V binding and SRB assay, statistical significance was evaluated using a one-tailed Student *t*-test. For animal testing, paired *t*-tests for comparisons between and within groups were used to determine the significance of the differences in tumor growth in vivo. Statistical significance was established at $p < 0.05$.

3. Results

3.1. Development of cell-permeable endostatin proteins

Hydrophobic macromolecule transduction domains (MTDs) have been used to deliver a variety of protein cargoes to mammalian cells and tissues. Similarly, MTD56 and MTD73 were found to enhance the uptake of a His-tagged enhanced green fluorescent protein (EGFP) in RAW cells as assessed by flow cytometry (Supporting Information Fig. S1A). The uptake of EGFP proteins containing either MTD56(HM_{56}E) or MTD73(HM_{73}E)was greater than a similarly configured protein containing the membrane translocation sequence (MTS) from FGF4 [40]. Similar results were obtained in NIH3T3 cells, using fluorescent microscopy to monitor protein uptake; whereas, only minimal levels of protein uptake were observed with a protein (HE) lacking a MTD sequence (Supporting Information Fig. S1B). MTD sequences also enhanced protein delivery to a variety of tissues in mice after I.P. administration, although HM_{56}E and HM_mE displayed greater tissue distribution than HM_{73}E particularly in the heart, lung and brain (Supporting Information Fig. S1C).

MTD56 or MTD73 were subsequently tested for the ability to enhance cellular Endostatin (ES) uptake. His-tagged ES proteins (HES) containing either MTD56 or MTD73 (Fig. 1A, upper panels) were expressed in *E. coli* (Fig. 1A, lower panels), purified under denaturing conditions by Ni^{2+}-affinity chromatography, refolded, labeled with FITC, and protein uptake was tested either in NIH3T3 cells by fluorescent confocal microscopy (Fig. 1B) orin RAW cells by flow cytometry (Fig. 1C). Enhanced levels of protein uptake were observed with ES proteins containing MTD56 positioned on either the N- (HM_{56}ES) or C-terminus ($HESM_{56}$),or with endostatin modified by an N-terminal MTD73 sequence (HM_{73}ES). A protein ($HM_{56}ESM_{56}$) containing MTD56 on both ends was less active. Similar results were obtained in RAW cells, in which HM_{73}ES displayed the greatest levels of protein uptake as assessed by flow cytometry (Fig. 1C).

Since HM_{73}ESentered cells efficiently and produced the highest yields of soluble protein when expressed in *E. coli* (Fig. 1A), we monitored systemic delivery of the protein (after I.P. administration) in a variety of murine tissues, including subcutaneous tumors of HCT116 cells xenografted on nude mice. MTD73 enhanced the systemic delivery of ES protein to all tissues examined (liver, kidney, spleen, lung, heart and brain), including subcutaneous HCT116 tumor xenografts (Fig. 1D). By contrast, His-tagged ES withoutan MTD sequence (HES) did not accumulate in any of the distal tissues or tumors examined (Fig. 1D). These results establish MTD73 as a vehicle for intracellular ES delivery, both in vitro and in vivo.

In addition to MTD56 (VLLAAALIA) and MTD73 (PVLLLLA), we evaluated ES proteins containing 6 other MTDs (18, 41, 66, 85, 135 and 159), but the proteins were less soluble, produced lower yields when expressed in *E. coli* and entered cells less efficiently (data not shown); therefore, these proteins were not evaluated further.

3.2. Inhibition of angiogenesis-associated phenotypes by cell-permeable endostatin

Having developed cell permeable (CP) ES proteins with enhanced capacity to enter cells, we tested the relationship

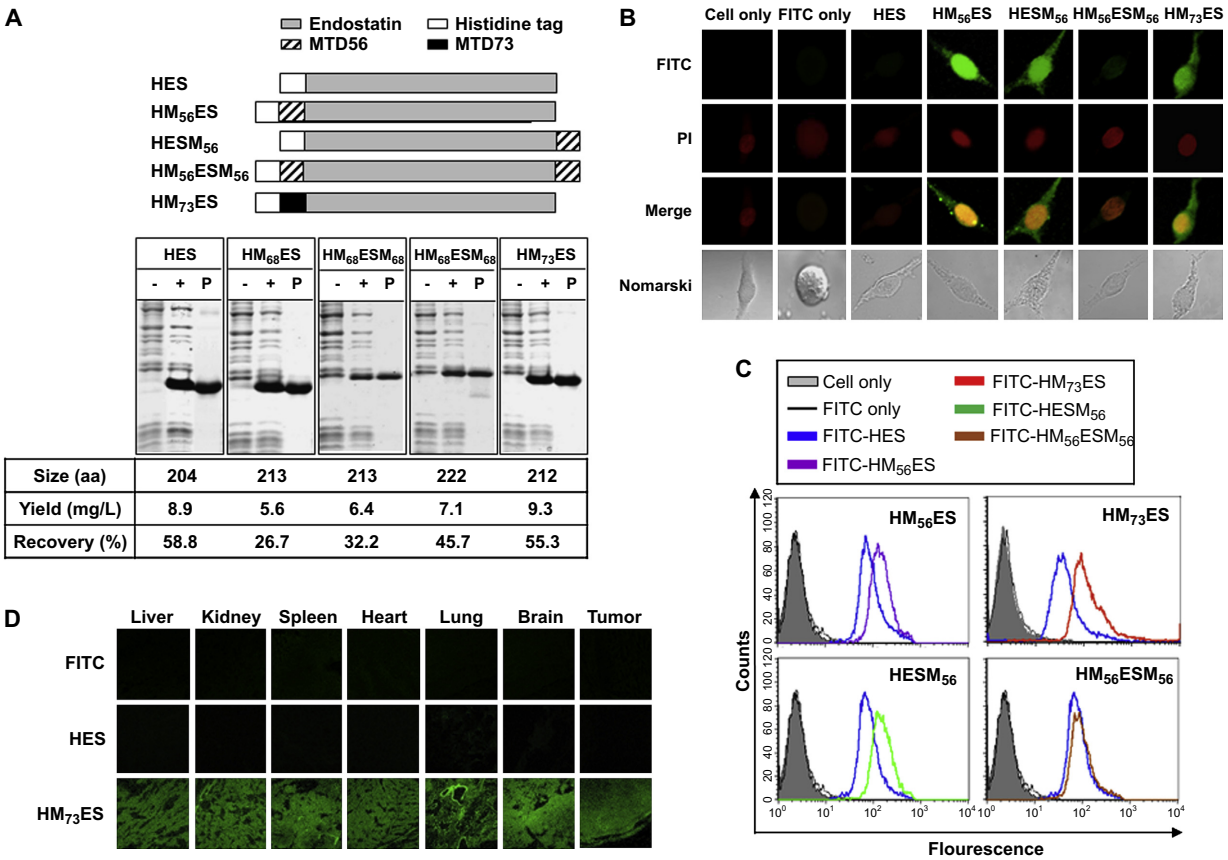

Size (aa)	204	213	213	222	212
Yield (mg/L)	8.9	5.6	6.4	7.1	9.3
Recovery (%)	58.8	26.7	32.2	45.7	55.3

Fig. 1. Structure, purification and intracellular delivery of recombinant endostatin proteins. (A) Structure of recombinant endostatin proteins fused to MTD56 or MTD73 and their expression and purification. The expression of proteins before (−) and after (+) induction with IPTG and the purified yield (P) were monitored. H, M and ES denote 6xHis tag (▭), MTD (MTD56: ▨ and MTD73: ■) and endostatin (▭) sequences, respectively. The size (aa: number of amino acids) and yield (mg/L) are indicated. Recovery refers to the percentage of extracted protein obtained in soluble form after refolding. (B and C) Intracellular protein delivery. NIH3T3 or RAW 264.7 cells were incubated with 10 μM of FITC-conjugated recombinant proteins, 10 μM unconjugated FITC (FITC only) or culture medium (Cell only) for 1 h, were treated with proteinase K to remove non-internalized protein and visualized by confocal microscopy (B) or flow cytometry (C), respectively. (D) MTD-mediated systemic ES delivery to murine tissues. Cryosections (15 μm) of saline-perfused organs were prepared from mice 2 h after intraperitoneal injection of 10 μg FITC or 300 μg FITC-labeled ES proteins with ($HM_{73}ES$) or without (HES) the MTD73 sequence. Tissue distribution of the recombinant proteins was assessed by fluorescence microscopy.

between enhanced uptake and several biological activities associated with the protein. Initial studies examined the effects of CP-ES on a variety of biomarkers including: β-Catenin, c-Myc, STAT3 (signal transducer and activator of transcription 3); VEGF (vascular endothelial cell growth factor) and pERK (phosphorylated extracellular signal-regulated kinase). Human vascular endothelial cells (HUVECs) were treated with 10 μM of CP-ES containing MTD56 ($HM_{56}ES$, $HESM_{56}$ and $M_{56}ESM_{56}$),MTD73 ($HM_{73}ES$) or control ES lacking an MTD (HES) for 1 h and biomarker expression was monitored after 2 (pERK), 8 (β-Catenin and STAT3) or 12 h (c-Myc and VEGF) by immunoblot analysis (Fig. 2A). $HM_{73}ES$ was the most active protein tested, suppressing proliferation- (c-Myc), signaling- (β-Catenin, STAT3 and pERK) and angiogenesis- (VEGF)associated markers. These results are consistent with data from Fig. 1 and Supplementary Fig. S1 in which $HM_{73}ES$ displayed the highest solubility, and cell and tissue permeability of the MTD-fused proteins tested. Therefore, studies to compare the anti-angiogenic potential of ES and CP-ES focused on $HM_{73}ES$ and the identical protein that lacks an MTD sequence, HES.

We compared the ability of HES and $HM_{73}ES$to suppress capillary tube formation in an in vitro model of angiogenesis. HUVECs spontaneously align and form hollow, branched tubes when cultured in matrigel-containing media (Fig. 2B). Treatment with 2.5 or 5 μM HES for 16 h resulted in a significant (20–24%; $p < 0.01$) suppression of tube formation (Fig. 2B), as assessed by counting the number of branch points in a8.96 cm^2 area (Fig. 2C). CP-ES was a more potent inhibitor of endothelial tube formation—63% and 82% ($p < 0.001$) in cells treated with 2.5 or 5 μMHM$_{73}$ES, respectively (Fig. 2C). Differences between HES and $HM_{73}ES$ were maintained even at protein concentrations up to 20 μM (Supporting Information Fig. S2). Branching was completely blocked by $HM_{73}ES$ at concentrations of 10 μM or higher.

3.3. Enhanced suppression of angiogenesis-associated phenotypes by CP-ES

In principle, the results obtained in the tube formation assay could reflect differences in cell migration, proliferation or survival. To examine these issues further, we used a wound-healing assay to compare the effects of HES and $HM_{73}ES$ on cell proliferation and/or migration. Specifically, HUVEC monolayers were treated with recombinant proteins for 2 h and then wounded, and the ability of the cells to repopulate the wounded area was monitored for 24 h (Fig. 3A, left panel). HES and $HM_{73}ES$ both suppressed repopulation of the wounded monolayer; however, $HM_{73}ES$ had the greatest effect—93% ($p < 0.001$) as compared to untreated controls (Fig. 3A). In comparison, HES suppressed wound healing to a lesser extent (42%; $p < 0.01$). Similar results were obtained in cell proliferation

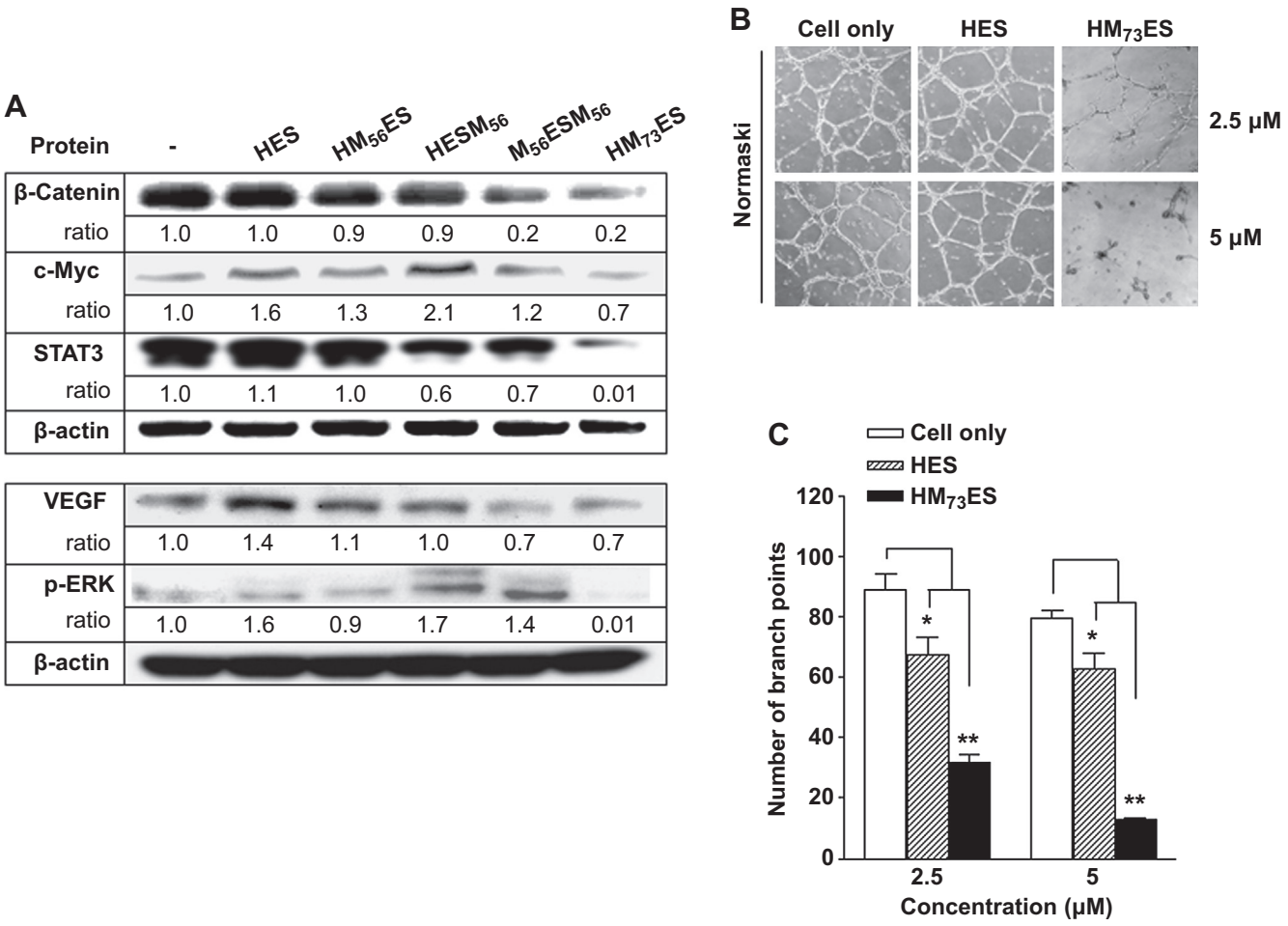

Fig. 2. Enhanced activity of cell-permeable endostatin on endothelial cell biomarker expression and tube formation. (A) Western blot analyses. HUVECs were treated for 1 h with 10 μM recombinant endostatin proteins containing MTD56 ($HM_{56}ES$, $HESM_{56}$ or $HM_{56}ESM_{56}$), MTD73 ($HM_{73}ES$) or lacking an MTD sequence (HES). The cells were incubated for an additional 2, 8 or 12 h in growth medium and analyzed for β-Catenin, c-Myc, p-ERK, STAT3, β-actin, VEGF, and phosphorylated ERK (p-ERK) expression. (B) Endothelial tube forming assay. HUVECs were treated with 2.5 or 5 μM protein (HES or $HM_{73}ES$) for 16 h and observed microscopically (top panel). The number of branch points in an 8.9 cm^2 area (mean ± S.D., 3 experiments) were plotted (lower panel). $^{*}p < 0.01$; $^{**}p < 0.001$, as determined by a Student unpaired *t*-test.

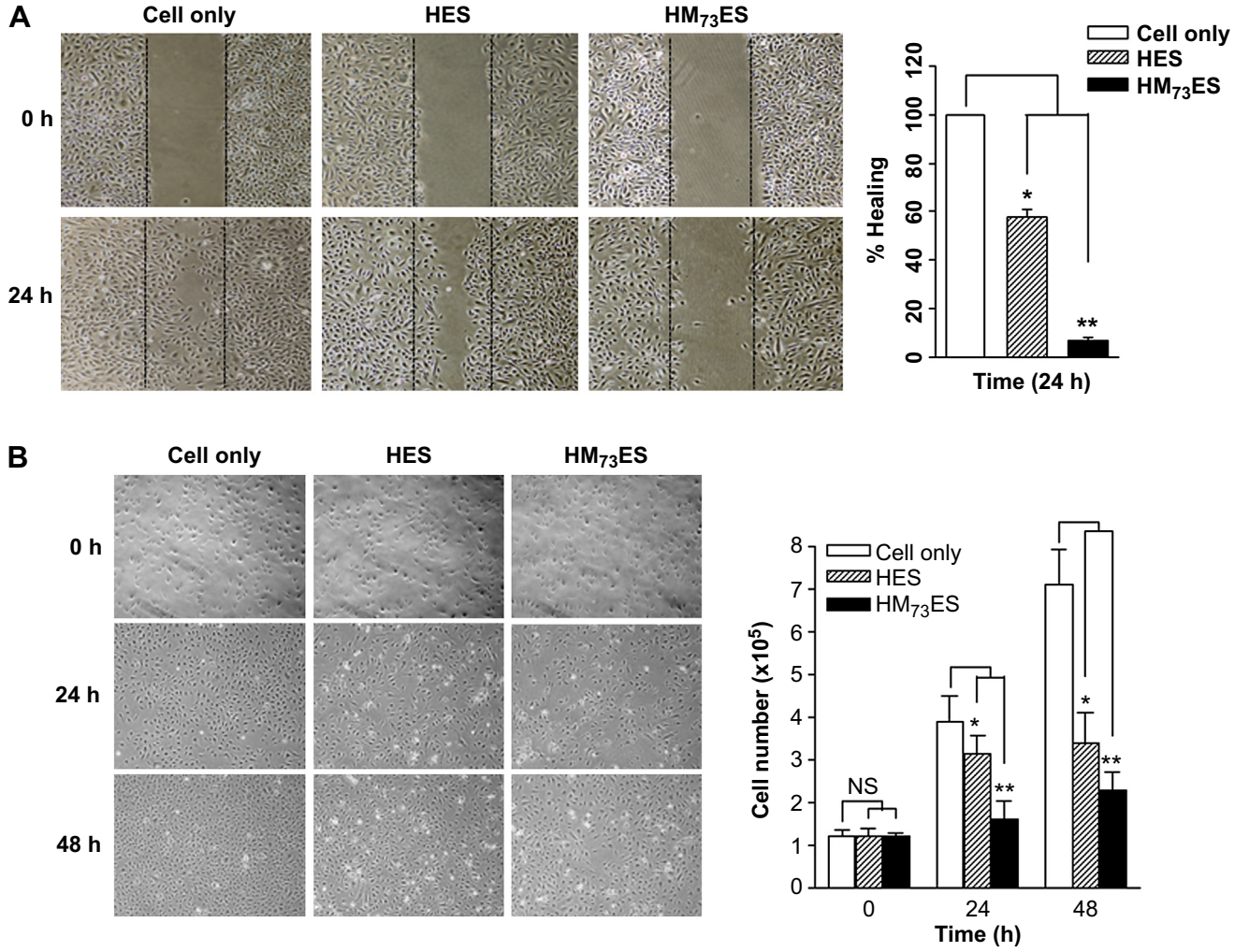

Fig. 3. Enhanced activity of cell-permeable endostatin in wounded monolayer and cell proliferation assays. (A) Wound healing assay. HUVEC monolayers were treated with 10 μM HES or $HM_{73}ES$ for 1 h in serum-free media, photographed after an additional 24 h in normal growth media (left panel) and cell coverage over the "wound" areas was quantified (mean ± S.D., 3 experiments; right panel). (B) Cell proliferation assay. HUVECs plated the day before were treated with 10 μM HES or $HM_{73}ES$ for 1 h in serum-free medium and cultured for 24 or 48 h in growth media. The cells were photographed (left panel) and counted (right panel). $^{*}p < 0.01$; $^{**}p < 0.001$, as determined by a Student unpaired *t*-test.

assays (Fig. 3B). Treatment of HUVECs with 10 μM of $HM_{73}ES$ for 2 h inhibited their proliferation after 24 and 48 h by 60% and 71% ($p < 0.001$), respectively. By comparison, HES inhibited HUVAC proliferation by 20% and 52% ($p < 0.01$) over the same time intervals.

We also compared the ability of ES and CP-ES to induce apoptosis after treating HUVECto 2 μM protein for 24 or 48 h. The MTD containing endostatin ($HM_{73}ES$) was a more potent inducer of apoptosis in HUVAC cells, as assessed by the accumulation of cells with sub-G_1 DNA content (Fig. 4A, left panel). In addition, apoptosis was also examined in a variety of cell lines, including endothelial cells, tumor cells and untransformed cells, by changes in annexin V staining. Cells were treated with 5 μM HES or $HM_{73}ES$ in serum-free media for varying times [HUVEC: 7 h (Fig. 4B); A549:1, 3 and 5 h (Fig. 4C); MDA-MB-231, HCT116 and NIH3T3: 3 h (Fig. 5A)]. With the exception of NIH3T3 cells (Fig. 5A), $HM_{73}ES$ was a more potent inducer of apoptosis than either HES or vehicle alone (i.e. exposure of cells to serum-free media without recombinant proteins). In addition, $HM_{73}ES$ treatment altered the morphologies of HUVECs and A549 cells (lower panels in Fig. 4B and C), consistent with higher levels of apoptosis.However, neither recombinant ES appeared to induce apoptosis in NIH3T3 cells (Fig. 5A); nor was cell viability affected, as measured by sulforhodamine B (SRB) staining, even after exposing NIH3T3 cells to higher concentrations (10 μM)of ES proteins over 8 h (Fig. 5B). This suggests neither protein is overtly toxic to cells. Together, the data from Figs. 2–5 indicate CP-ES has a greater ability than ES to inhibit multiple angiogenesis-associated phenotypes in endothelial cells, including biomarker expression, proliferation, migration, survival, and tube formation.

3.4. CP-ES has enhanced anti-tumor and anti-angiogenic activities

We next compared the anti-tumor activities of ES and CP-ES against human cancer xenografts. HCT116 colorectal tumor cells were injected subcutaneously into nude mice, tumors were allowed to grow to 60–80 mm^3 in size, and then the mice were injected subcutaneously with 200 μg/mouse HES or $HM_{73}ES$ or with diluent alone (PBS) every day for 3 weeks. The mice were monitored for an additional 2 weeks after treatments ended (Fig. 6A). The CP-ES suppressed tumor growth to a much greater extent than the protein lacking an MTD sequence (79%vs. 22% after 21 days) as compared to tumors treated with diluent alone, and the difference persisted to day 35 (66% vs. 20%). Differences in tumor size were apparent by external examination (Fig. 6B) and after the

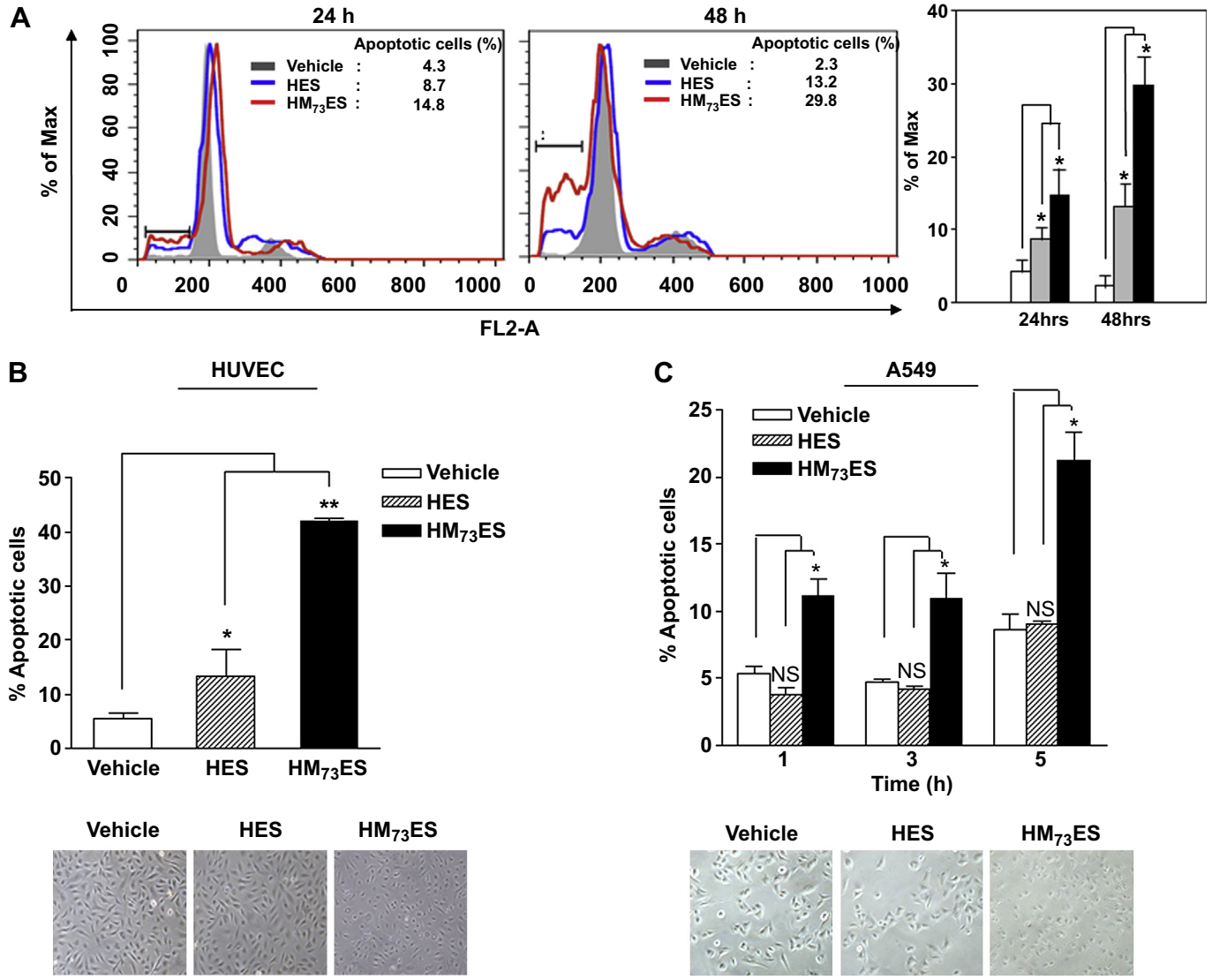

Fig. 4. Enhanced apoptosis in endothelial cells exposed to cell-permeable endostatin. (A) DNA content analysis. HUVECs were treated with 2 μM of protein for 24 or 48 h (gray filled: vehicle, blue line: HES and red line: $HM_{73}ES$), stained with propidium iodide and analyzed by flow cytometry. Cells with less than G_1 DNA content plotted (right panel) were regarded as apoptotic cells; $^{*}p < 0.01$; $^{**}p < 0.001$, as determined by a Student unpaired *t*-test. (B and C) apoptosis in human vascular endothelial cells, HUVEC (B) and A549 colon cancer cells (C). Cells treated for 48 h with 2 μM of the indicated recombinant ES were stained with annexin V and percentage of cells staining with annexin V (% apoptotic cells) is plotted (upper panels); $^{*}p < 0.01$; $^{**}p < 0.001$, as determined by a Student unpaired *t*-test. Lower panels show photomicrographs of cells after protein treatment. NS = not significant. (For interpretation of the references to color in this figure legend, the reader is referred to the web version of this article.)

tumors were excised from the animal (Fig. 6C) and weighed (Fig. 6C). Differences in tumor size/weight between control and $HM_{73}ES$-treated mice were statistically significant even at day 21 ($p < 0.05$). None of the protein-treated mice displayed loss of body weight as compared to controls (data not shown), suggesting the proteins were well-tolerated.

Tumor vascularization was also assessed in sections from day 21 tumors by immunostaining for the vascular endothelial cell–specific marker 4A11 (Fig. 6D, top panel). The vasculature within tumors from $HM_{73}ES$-treated mice was markedly under-developed as compared to tumors from control or HES-treated mice. H&E stained sections (Fig. 6D, bottom panel) from $HM_{73}ES$-treated tumors also showed prominant regions of necrosis and/or apoptosis.

Similar results were obtained using different protein preparations (Supporting Information Fig. S3A) or a different (A549) tumor xenograft model (Supporting Information Fig. S3B). In these experiments the HES protein inhibited HCT116 tumor growth as compared to controls by 38% and 40% at day 21 and 35, respectively, and A549 tumor growth by 62% and 67% over the same intervals. In each case, $HM_{73}ES$ outperformed HES—inhibiting HCT116 tumor growth by 91% and 62% at day 21 and 35, respectively, and A549 tumor growth by 89% and 83% over the same intervals. Protein treatment did not affect mouse body weight or noticeable changes in behavior, food/water consumption or movement/activity, suggesting the proteins were well-tolerated, at least in these short-term animal tests.

4. Discussion

After the discovery of endostatin (ES) as an angiogenesis inhibitor and the accompanying demonstration of anti-tumor activity [5], ES moved quickly into clinical trials [1]. However, within five years U.S. trials were discontinued due to problems with protein formulation and insufficient therapeutic response. Clinical development has been further stymied by insufficient understanding of ES function and the mechanism by which ES targets tumor

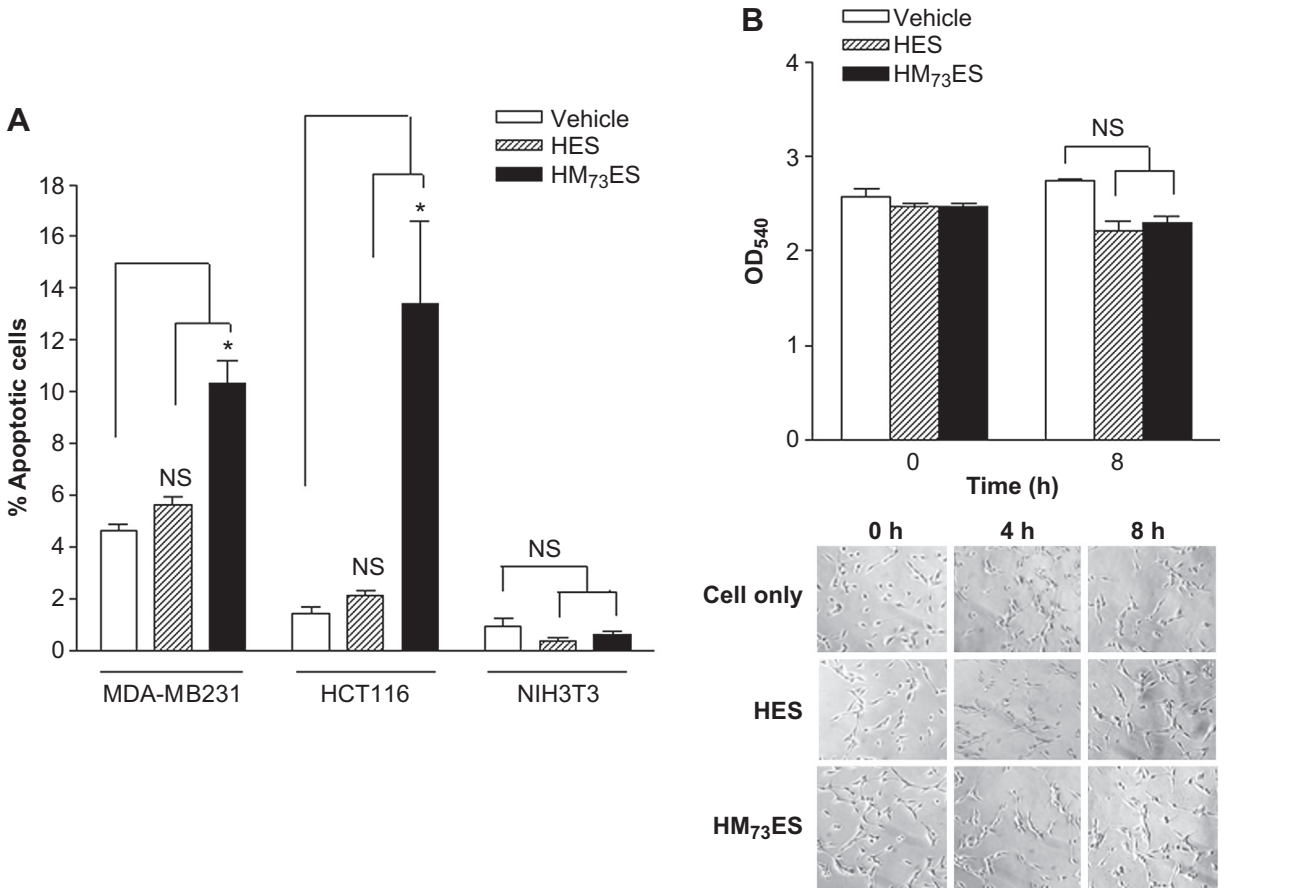

Fig. 5. Sensitivity of different cell lines to ES-induced apoptosis. (A) Human tumor cell lines and NIH3T3 cells have different sensitivity to recombinant ES. Human breast (MDA-MB-231) and colon (HCT116) cancer cells and mouse NIH3T3 cells were treated for 3 h with 5 μM of the indicated protein (HES: hatched bar and $HM_{73}ES$: black bar) or vehicle (culture medium: white bar) and the percent of apoptotic cells was assessed by annexin-V staining. (B) NIH3T3 cell viability. NIH3T3 cells were treated 10 μM protein (HES or $HM_{73}ES$) for 8 h and stained with sulforhodamine B. None of the treatments appeared toxic as assessed by measuring absorbance at 540 nm (upper panel) or cell appearance (lower panels). The data are means ± S.D. of triplicate experiments. $^{*}p < 0.01$ as determined by unpaired Student's *t*-test.

angiogenesis. The present study investigated the effect of enhanced cytoplasmic protein uptake on the biological activities of ES. Specifically, we developed a cell-permeable ES ($HM_{73}ES$) with enhanced capacity to enter cells by adding a macromolecule transduction domain (MTD). We then showed that $HM_{73}ES$ inhibited angiogenesis-associated phenotypes in cultured endothelial cells and suppressed the growth of human tumor xenografts to a significantly greater extent than ES lacking the MTD sequence. These results suggest, first, much of the activity of ES against tumors depends on one or more intracellular functions, and second, the potential anti-tumor activities of native ES are intrinsically limited at the level of cellular uptake and/or intracellular localization.

Our approach exploited the ability of hydrophobic MTD sequences, derived from the signal peptides of secreted and transmembrane proteins, to promote bidirectional transfer of peptides and proteins across the plasma membrane [31–33]. MTD sequences have been used to deliver peptides and proteins systemically to a variety of tissues and thereby protect animals against lethal inflammatory diseases [34–37,41], suppress pulmonary metastases [38] and inhibit subcutaneous tumor xenografts [31,39]. As with other MTD sequences, the development of MTD73 had a large empirical component, starting with a screen for EGFP reporter protein uptake. The sequence was further modified to eliminate charged and polar amino acids, increase predicted α-helical content and limit the number of consecutive hydrophobic residues. Finally, of the 8 MTDs tested, ES fusion proteins containing MTD73 displayed the best combination of protein solubility, purification yield and uptake of FITC-labeled ES by cells and tissues. Based on relative fluorescence, MTD73 appeared to enhance ES uptake in cultured cells (HUVEC, RAW and NIH3T3 cells)and animal tissues (liver, kidney, spleen, heart, lung, brain and tumor xenografts) by at least 5-fold.

$HM_{73}ES$and HES suppressed multiple angiogenesis-associated phenotypes in cultured HUVACs including tube formation, wound-healing, cell proliferation and survival [7,11,42]. These effects were accompanied by reductions in MAPK signaling (ERK phosphorylation), and in β-Catenin, c-Myc, STAT3, and VEGF protein expression–consistent with previously described effects of ES [13,15,43–45]. In each case, cell-permeable ES ($HM_{73}ES$) heightened all of the effects associated with the control ES protein (HES).

We were unable to assess potential contributions of the MTD sequence on the biological activity of CP-ES due to problems expressing MTD sequences in soluble form. However, we have observed no effects in cells or tissues treated with non-functional cargos, e.g. EGFP, containing MTD sequences (Fig. 1 and Fig. S1) [31,35,38,39]. Moreover, all of the biological effects attributed to CP-ES were qualitatively similar to those observed with the Endostatin sequence alone; the MTD appeared only to enhance the magnitude of the effects.

Our results support earlier studies that proposed protein internalization as an important if not essential feature of protein activity

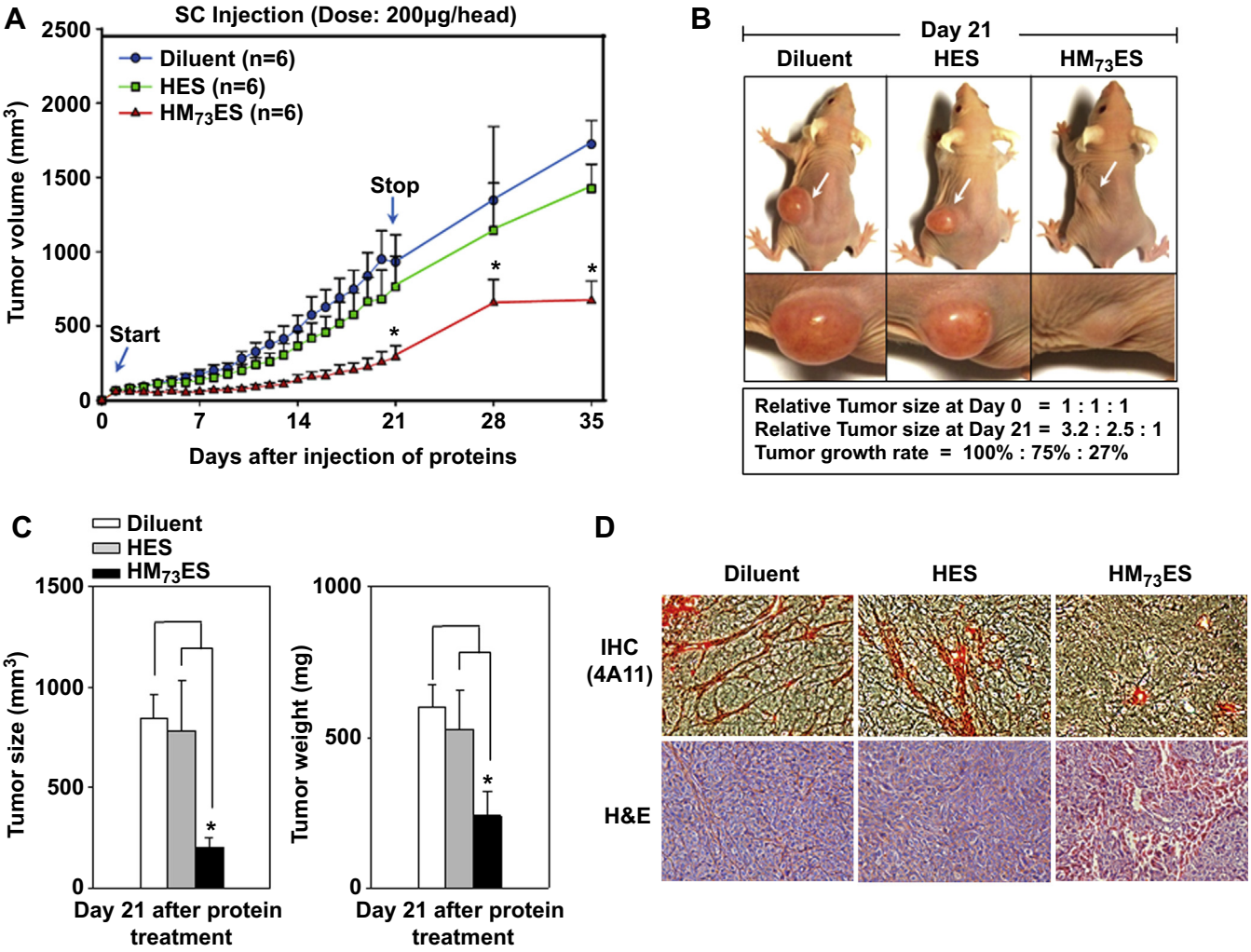

Fig. 6. CP-endostatin inhibits tumor growth by inhibiting angiogenesis. (A) Inhibition of tumors induced by subcutaneous injection of HCT116 colorectal tumor cells. After tumors reached a size of 60–80 mm^3 (start) the mice were injected daily (subcutaneously) for three weeks with diluent alone (blue circles) or with 200 μg HES (green squares), or $HM_{73}ES$ (red triangles). Tumor growth was suppressed to varying degrees after protein therapy ended (stop). $^*p < 0.05$ as determined by Student's *t*-test. (B) External appearance of tumor bearing mice. Representative mice treated with diluent, HES or $HM_{73}ES$ were photographed 21 days after starting protein therapy. (C) Tumor size. The volumes (left panel) and weights (right panel) of tumors dissected 21 days after treatment are plotted. The data are means ± S.D. ($n = 6$). $^*p < 0.05$ as determined by unpaired Student's *t*-test. (D) Tumor histology. Tumor sections (5 μm) from tumors obtained after 21 days of protein treatment were immunostained with the vascular endothelial cell–specific antibody 4A11 plus horse radish peroxidase conjugated secondary antibody, visualized with diaminobenzidine tetrahydrochloride, and counterstained with eosin (upper panels). Sections were also stained with hematoxylin and eosin (H&E, lower panels). (For interpretation of the references to color in this figure legend, the reader is referred to the web version of this article.)

[7,9,18,21,22]. Default pathways mediating ES uptake are known to require arginine-rich sequences that also mediate low affinity interactions with heparin sulfate proteoglycans and integrins [8,10,11,24,25]. Unfortunately, with proteins such as ES, protein uptake is difficult to study in cells exposed to concentrations of recombinant proteins high enough to saturate abundant, relatively low-affinity binding sites. The analysis itself is subject to a variety of artifacts that make it difficult to distinguish between cell-associated and internalized proteins [27,46]. Moreover, many basic proteins that bind heparin sulfate proteoglycans enter cells by caveolin-dependent and independent endocytosis [27], including cationic protein transduction domains, such as HIV-1 Tat [26]. The bulk uptake often exceeds and therefore masks a smaller, a biologically active component that enters the cytoplasm either by escaping the vesicular compartment or by alternative routes, e.g. one involving higher affinity (but less abundant) receptors. Inefficient cytoplasmic delivery would explain why relatively high concentrations of ES are required for biological activity [30]. Vesicular sequestration of basic proteins typically limits tissue penetration and bioavailability, thus hampering efforts to develop protein-based therapeutics [27].

In contrast to cationic protein transduction domains, hydrophobic MTD sequences appear to penetrate the plasma membrane directly [33] after inserting into the membranes [32]. MTD-facilitated uptake of larger protein cargoes is sensitive to low temperature, does not require microtubule function or utilize ATP, and intracellular accumulation requires an intact plasma membrane [31]. Cell-permeable $p18^{INK4c}$ traversed synthetic membranes consisting of cholesterol and phospholipid and was capable of bidirectional movement across membranes as assessed by cell-to-cell protein transfer [31]. Similarly, uptake of fluorescent $HM_{73}ES$ by cultured cells and widespread tissue distribution in animals after I.P. administration are consistent with enhanced cytoplasmic delivery and cell-to-cell transfer, as compared to the prototype ES (HES) that lackedan MTD sequence. In principle, cell-to-cell transfer should also reduce biphasic dose–response profiles observed with angiogenesis inhibitors (reviewed in Ref. [47]) as tissue penetration is expected to depend less on tumor vasculature.

Clinical trials using recombinant human ES show that the protein is tolerated at doses up to 240 mg/m^2. Although U.S. trials were discontinued due to poor clinical responses, a modified ES (designated ZBP-endostatin or Endostar®) is being evaluated in China, together with conventional chemotherapeutic agents [1,6]. ZBP-endostatin contains an amino-terminal 6xhistidine tag, generated by attaching a MGGSHHHHH sequence to the amino-terminal histidine of the native human ES sequence. This protein is reported to have higher anti-angiogenesis and anti-tumor activities than native ES in both laboratory and clinical settings. Proposed reasons for the difference include maintenance of N-terminal sequence integrity, enhanced zinc binding (although we observed no effect of Zn^{2+} on ES refolding or activity, data not shown), and improved solubility and/or recovery of *E. coli*–expressed recombinant proteins [6]. Our results suggest another mechanism to explain the enhanced activity of ZBP-ES as compared to native ES—enhanced protein uptake mediated by the amino-teminal 6x-histidine tag. L-histidine heptamers have been shown to interact with heparin sulfate proteoglycans [48] andenter cells [49]. In an earlier report, we showed that a 6xHis tag similar to the N-terminal Endostar® sequence significantly enhanced the intracellular delivery (but not enzymatic activity) of Cre recombinase [50] into Caveolin1-deficientlymphocytes [26]. Enhanced Cre uptake mediated by the 6xHis tag was comparable to the reported enhanced activity of Endostar® as compared to native ES [6].

5. Conclusion

The present study shows that cytoplasmic uptake of ES is an important functional determinant with regard to both angiogenesis and anti-tumor activity. Our results highlight the importance of as yet poorly understood intracellular targets of ES and suggest ways to improve ES-based cancer therapeutics.

Grant support

This work was supported by grant of the Industrial Strategic Technology Development Program (10032101 to D.J.) of Ministry of Knowledge Economy, Republic of Korea.

Disclosure any potential conflicts of interest

ProCell Therapeutics, Inc. and Daewoong Jo have filed patent for "cell-permeable endostatin recombinant protein, a polynucleotide encoding the same, and anti-cancer preparation containing the same as an active component" under the name of Daewoong Jo; JongMin Lee; Kyoungho Park; Minh Tam Duong. The relevant application number is PCT/KR2009/001726. There are no further patents, products in development or marketed products to declare. D. Jo was the founding scientist of ProCell Therapeutics, Inc., and is affiliated to Vanderbilt University at present. J. Lim and G. Lee are employees of ProCell Therapeutics, Inc. Hereby; these authors disclose a financial interest in the company. The other authors disclosed no potential conflicts of interest.

Acknowledgments

We thank Dr. Chris Ko for his critical comment and many young scientists including Dr. Jongmin Lee who were involved in the early stage of this study for their technical assistance.

Appendix A. Supplementary data

Supplementary data related to this article can be found online at http://dx.doi.org/10.1016/j.biomaterials.2013.05.011.

References

[1] Kessler T, Bayer M, Schwoppe C, Liersch R, Mesters RM, Berdel WE. Compounds in clinical phase III and beyond. Recent Results Cancer Res 2010;180:137–63.
[2] Samant RS, Shevde LA. Recent advances in anti-angiogenic therapy of cancer. Oncotarget 2011;2:122–34.
[3] Verheul HM, Pinedo HM. Possible molecular mechanisms involved in the toxicity of angiogenesis inhibition. Nat Rev Cancer 2007;7:475–85.
[4] Folkman J. Antiangiogenesis in cancer therapy–endostatin and its mechanisms of action. Exp Cell Res 2006;312:594–607.
[5] O'Reilly MS, Boehm T, Shing Y, Fukai N, Vasios G, Lane WS, et al. Endostatin: an endogenous inhibitor of angiogenesis and tumor growth. Cell 1997;88:277–85.
[6] Fu Y, Tang H, Huang Y, Song N, Luo Y. Unraveling the mysteries of endostatin. IUBMB Life 2009;61:613–26.
[7] Dixelius J, Larsson H, Sasaki T, Holmqvist K, Lu L, Engstrom A, et al. Endostatin-induced tyrosine kinase signaling through the Shb adaptor protein regulates endothelial cell apoptosis. Blood 2000;95:3403–11.
[8] Karumanchi SA, Jha V, Ramchandran R, Karihaloo A, Tsiokas L, Chan B, et al. Cell surface glypicans are low-affinity endostatin receptors. Mol Cell 2001;7:811–22.
[9] MacDonald NJ, Shivers WY, Narum DL, Plum SM, Wingard JN, Fuhrmann SR, et al. Endostatin binds tropomyosin. A potential modulator of the antitumor activity of endostatin. J Biol Chem 2001;276:25190–6.
[10] Rehn M, Veikkola T, Kukk-Valdre E, Nakamura H, Ilmonen M, Lombardo C, et al. Interaction of endostatin with integrins implicated in angiogenesis. Proc Natl Acad Sci U S A 2001;98:1024–9.
[11] Wickstrom SA, Alitalo K, Keski-Oja J. Endostatin associates with integrin alpha5beta1 and caveolin-1, and activates Src via a tyrosyl phosphatase-dependent pathway in human endothelial cells. Cancer Res 2002;62:5580–9.
[12] Urbich C, Reissner A, Chavakis E, Dernbach E, Haendeler J, Fleming I, et al. Dephosphorylation of endothelial nitric oxide synthase contributes to the anti-angiogenic effects of endostatin. FASEB J 2002;16:706–8.
[13] Hanai J, Dhanabal M, Karumanchi SA, Albanese C, Waterman M, Chan B, et al. Endostatin causes G1 arrest of endothelial cells through inhibition of cyclin D1. J Biol Chem 2002;277:16464–9.
[14] Lee SJ, Jang JW, Kim YM, Lee HI, Jeon JY, Kwon YG, et al. Endostatin binds to the catalytic domain of matrix metalloproteinase-2. FEBS Lett 2002;519:147–52.
[15] Kim YM, Hwang S, Kim YM, Pyun BJ, Kim TY, Lee ST, et al. Endostatin blocks vascular endothelial growth factor-mediated signaling via direct interaction with KDR/Flk-1. J Biol Chem 2002;277:27872–9.
[16] Sudhakar A, Sugimoto H, Yang C, Lively J, Zeisberg M, Kalluri R. Human tumstatin and human endostatin exhibit distinct antiangiogenic activities mediated by alpha v beta 3 and alpha 5 beta 1 integrins. Proc Natl Acad Sci U S A 2003;100:4766–71.
[17] Dixelius J, Cross MJ, Matsumoto T, Claesson-Welsh L. Endostatin action and intracellular signaling: beta-catenin as a potential target? Cancer Lett 2003;196:1–12.
[18] Shi H, Huang Y, Zhou H, Song X, Yuan S, Fu Y, et al. Nucleolin is a receptor that mediates antiangiogenic and antitumor activity of endostatin. Blood 2007;110:2899–906.
[19] Pollheimer J, Haslinger P, Fock V, Prast J, Saleh L, Biadasiewicz K, et al. Endostatin suppresses IGF-II-mediated signaling and invasion of human extravillous trophoblasts. Endocrinology 2011;152:4431–42.
[20] Zhang Y, Zhang J, Jiang D, Zhang D, Qian Z, Liu C, et al. Inhibition of T-type Ca(2)(+) channels by endostatin attenuates human glioblastoma cell proliferation and migration. Br J Pharmacol 2012;166:1247–60.
[21] Chen Y, Wang S, Lu X, Zhang H, Fu Y, Luo Y. Cholesterol sequestration by nystatin enhances the uptake and activity of endostatin in endothelium via regulating distinct endocytic pathways. Blood 2011;117:6392–403.
[22] Song N, Ding Y, Zhuo W, He T, Fu Z, Chen Y, et al. The nuclear translocation of endostatin is mediated by its receptor nucleolin in endothelial cells. Angiogenesis 2012;15:697–711.
[23] Hohenester E, Sasaki T, Olsen BR, Timpl R. Crystal structure of the angiogenesis inhibitor endostatin at 1.5 A resolution. EMBO J 1998;17:1656–64.
[24] Sasaki T, Larsson H, Kreuger J, Salmivirta M, Claesson-Welsh L, Lindahl U, et al. Structural basis and potential role of heparin/heparan sulfate binding to the angiogenesis inhibitor endostatin. EMBO J 1999;18:6240–8.
[25] Olsson AK, Johansson I, Akerud H, Einarsson B, Christofferson R, Sasaki T, et al. The minimal active domain of endostatin is a heparin-binding motif that mediates inhibition of tumor vascularization. Cancer Res 2004;64:9012–7.
[26] Wadia JS, Stan RV, Dowdy SF. Transducible TAT-HA fusogenic peptide enhances escape of TAT-fusion proteins after lipid raft macropinocytosis. Nat Med 2004;10:310–5.
[27] Fischer PM. Cellular uptake mechanisms and potential therapeutic utility of peptidic cell delivery vectors: progress 2001–2006. Med Res Rev 2007;27:755–95.
[28] Zhang AY, Yi F, Zhang G, Gulbins E, Li PL. Lipid raft clustering and redox signaling platform formation in coronary arterial endothelial cells. Hypertension 2006;47:74–80.
[29] Jin S, Zhang Y, Yi F, Li PL. Critical role of lipid raft redox signaling platforms in endostatin-induced coronary endothelial dysfunction. Arterioscler Thromb Vasc Biol 2008;28:485–90.
[30] Olsen BR. From the Editor's desk. Matrix Biol 2002;21:309–10.

[31] Lim J, Kim J, Duong T, Lee G, Kim J, Yoon J, et al. Antitumor activity of cell-permeable p18(INK4c) with enhanced membrane and tissue penetration. Mol Ther 2012;20:1540–9.
[32] Ramamoorthy A, Kandasamy SK, Lee DK, Kidambi S, Larson RG. Structure, topology, and tilt of cell-signaling peptides containing nuclear localization sequences in membrane bilayers determined by solid-state NMR and molecular dynamics simulation studies. Biochemistry 2007;46:965–75.
[33] Veach RA, Liu D, Yao S, Chen Y, Liu XY, Downs S, et al. Receptor/transporter-independent targeting of functional peptides across the plasma membrane. J Biol Chem 2004;279:11425–31.
[34] Liu D, Liu XY, Robinson D, Burnett C, Jackson C, Seele L, et al. Suppression of *Staphylococcal Enterotoxin* B-induced toxicity by a nuclear import inhibitor. J Biol Chem 2004;279:19239–46.
[35] Jo D, Liu D, Yao S, Collins RD, Hawiger J. Intracellular protein therapy with SOCS3 inhibits inflammation and apoptosis. Nat Med 2005;11:892–8.
[36] Liu D, Zienkiewicz J, DiGiandomenico A, Hawiger J. Suppression of acute lung inflammation by intracellular peptide delivery of a nuclear import inhibitor. Mol Ther 2009;17:796–802.
[37] Moore DJ, Zienkiewicz J, Kendall PL, Liu D, Liu X, Veach RA, et al. In vivo islet protection by a nuclear import inhibitor in a mouse model of type 1 diabetes. PLoS One 2010;5:e13235.
[38] Lim J, Jang G, Kang S, Lee G, Nga do TT, Phuong do TL, et al. Cell-permeable NM23 blocks the maintenance and progression of established pulmonary metastasis. Cancer Res 2011;71:7216–25.
[39] Lim J, Duong T, Do N, Do P, Kim J, Kim H, et al. Anti-tumor activity of cell-permeable RUNX3 protein in gastric cancer cells. Clin Cancer Res 2013;19:680–90.
[40] Hawiger J. Noninvasive intracellular delivery of functional peptides and proteins. Curr Opin Chem Biol 1999;3:89–94.
[41] Liu XY, Robinson D, Veach RA, Liu D, Timmons S, Collins RD, et al. Peptide-directed suppression of a pro-inflammatory cytokine response. J Biol Chem 2000;275:16774–8.
[42] Kuo CJ, LaMontagne Jr KR, Garcia-Cardena G, Ackley BD, Kalman D, Park S, et al. Oligomerization-dependent regulation of motility and morphogenesis by the collagen XVIII NC1/endostatin domain. J Cell Biol 2001;152:1233–46.
[43] Shichiri M, Hirata Y. Antiangiogenesis signals by endostatin. FASEB J 2001;15:1044–53.
[44] Hanai J, Gloy J, Karumanchi SA, Kale S, Tang J, Hu G, et al. Endostatin is a potential inhibitor of Wnt signaling. J Cell Biol 2002;158:529–39.
[45] Abdollahi A, Hahnfeldt P, Maercker C, Grone HJ, Debus J, Ansorge W, et al. Endostatin's antiangiogenic signaling network. Mol Cell 2004;13:649–63.
[46] Lundberg M, Johansson M. Is VP22 nuclear homing an artifact? Nat Biotechnol 2001;19:713–4.
[47] Javaherian K, Lee TY, Tjin Tham Sjin RM, Parris GE, Hlatky L. Two endogenous antiangiogenic inhibitors, endostatin and angiostatin, demonstrate biphasic curves in their antitumor profiles. Dose Response 2011;9:369–76.
[48] Lacy HM, Sanderson RD. 6xHis promotes binding of a recombinant protein to heparan sulfate. Biotechniques 2002;32. 254, 6, 8.
[49] Mitchell DJ, Kim DT, Steinman L, Fathman CG, Rothbard JB. Polyarginine enters cells more efficiently than other polycationic homopolymers. J Pept Res 2000;56:318–25.
[50] Lin Q, Jo D, Gebre-Amlak KD, Ruley HE. Enhanced cell-permeant Cre protein for site-specific recombination in cultured cells. BMC Biotechnol 2004;4:25.